



# A PC-ICCD for fast optical photometry

M. Uslenghi, M. Fiorini, G. Sarri

Istituto di Astrofisica Spaziale e Fisica cosmica, sez. Milano, via E. Bassini 15, 20133 Milano

## Abstract.

The availability of high-speed data from high-energy satellites (in particular RXTE) allowed investigating phenomena on time scales much faster than those accessible with the CCD, the astronomical detector for the optical range *par excellence*. That resulted in a rising interest for optical detectors able to perform observations coordinated with X and  $\gamma$ -Ray instruments and with similar time resolution.

In this context, we developed a detector based on a Photon Counting Intensified CCD optimized for the optical range, with format  $2048 \times 2048$  pixels and time resolution down to 4.5 ms. The detector has been calibrated at the 182 cm Asiago Cima Ekar telescope. Some results of the observations carried out have been reported in this paper.

**Key words.** Photon counting detectors – high speed photometry – FPGA

## 1. Introduction

High time resolution observations are an important subject for astrophysics, allowing investigating short time scale variations, periodic or quasi-periodic, occurring in a great variety of sources: cataclysmic variables, X-Ray binaries, flare stars, pulsars, AGN. Moreover, when coupled with imaging capability, they can provide a straightforward method to identify optical counterparts of X-Ray binary systems and gamma-ray sources.

The availability of high-speed data from high-energy satellites (in particular RXTE) allowed investigating phenomena on time scales much faster than those accessible with the CCD, the astronomical detector for the optical range *par excellence*. That resulted in a rising

interest for optical detectors able to perform observations coordinated with X and  $\gamma$ -Ray instruments and with similar time resolution.

In this context, we developed a Photon Counting Intensified CCD (PC-ICCD) optimized for the optical range, with format  $2048 \times 2048$  pixels and time resolution down to 4.5 ms on a reduced Field of View (16 ms full FOV). PC-ICCDs belong to the class of Microchannel Plates (MCP) based detectors, which can provide very high time resolution along with imaging capability. Largely used in Ultraviolet Astronomy, for optical observations the MCP limited dynamic range is a weak point. Generally, the readout systems of such devices are optimized for point-like response or for global dynamic range, but optical Astronomy requires high performance on both the figures of merit. In fact, wide dynamic range in response to a point-like source is needed in order to preserve the linearity of

---

Send offprint requests to: M. Uslenghi, [uslenghi@mi.iasf.cnr.it](mailto:uslenghi@mi.iasf.cnr.it)

Correspondence to: via E. Bassini 15, 20133 Milano

the detector in a large range of magnitude. In the mean time, high global maximum rate is important not to saturate the detector with the sky background.

Among the MCP readout systems, not only the CCD can provide the highest spatial resolution, but, more important, since the geometry is fixed by the physical 2-d array of the pixels on the sensor, no geometric distortion on large scale is present, not even at high count rate. Unlike systems where the number of readout channels is reduced by codifying the anodes (e.g. MAMA) or using the drift time of the signals to recover coordinates information (e.g. Delay Lines), time coincidence does not result in misallocation of photons, thus the maximum sustainable global count rate can be higher. Moreover, we developed a highly parallel real time processing electronics, based on Field Programmable Gate Array (FPGA) technology (Bergamini et al. 2000), not to limit the dynamic performance of the detector (see Uslenghi et al. 2004, for reference).

## 2. Detector Overview

The PC-ICCD is a photon counting detector based on a high-gain MCP image intensifier as input device. The intensifier in use is a sealed Z-stack of 25 mm diameter plates with  $10\ \mu\text{m}$  pores at  $12\ \mu\text{m}$  pitch, with a S20 photocathode. The intensifier virtually converts each photon, interacting photoelectrically with the photocathode, into a luminous spot on the phosphor screen that preserves the  $(x,y)$  location of the event. The photon event produced by the phosphor screen is reimaged onto the CCD chip by means of a fiber optic taper with a 1:2.4 demagnification ratio. The CCD camera subsequently detects the location of each event, whose centroid coordinates are determined in real-time with sub pixel accuracy. A digital electronics unit (Bergamini et al. 2000), based on Xilinx FPGAs, analyzes in real time each CCD frame to search for valid events (i.e. light spots produced by primary photoelectrons). A 2 Gbits/s fiber optic link based on the S-LINK Hola device connects the detector head with the digital electronics. The PC I/O is performed by a PCI I/O board (National Instruments PCI-

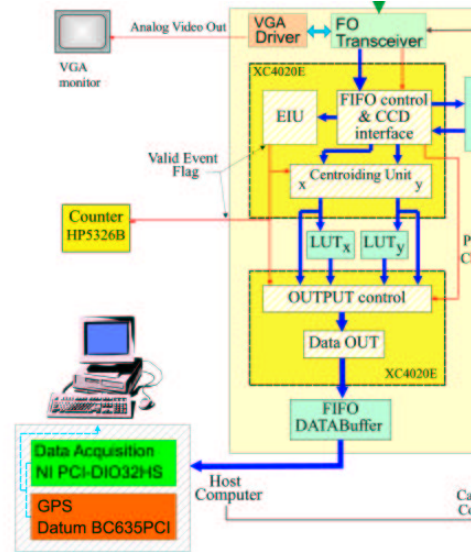


**Fig. 1.** Block diagram of the detector system.

DIO-32HS). A GPS board from Datum provides absolute timing with  $1\ \mu\text{s}$  accuracy, allowing to correlate optical observations with X and  $\gamma$ -Ray satellites. A scheme of the system is shown in Fig.1.

### 2.1. Software

Basic functions of detector management and data acquisition operations have been implemented in two DLL (Dynamic-Link Library), developed in Borland C++ 5.1. A Graphical User Interface has been developed in the Interactive Data Language (IDL) environment. A library of IDL routines is available to perform the data analysis. Exploiting the timing information, the software can also recenter the photons in order to compensate for small tracking errors.

## 3. Astronomical Observations

In order to assess the performance of the detector in astronomical applications, we carried out a 4-nights campaign at the 182 cm telescope of the Asiago Observatory - Cima Ekar. We observed several standard photometric stars, cho-

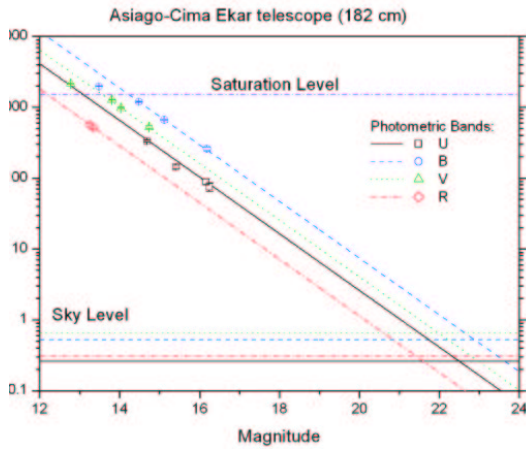


**Fig. 2.** Calibration of the detector in the Johnson photometric system (count rates are reported to the zenith). Note that the saturation level refers to the full FOV mode, whereas it is 4 times higher for a FOV reduced to 1/4.

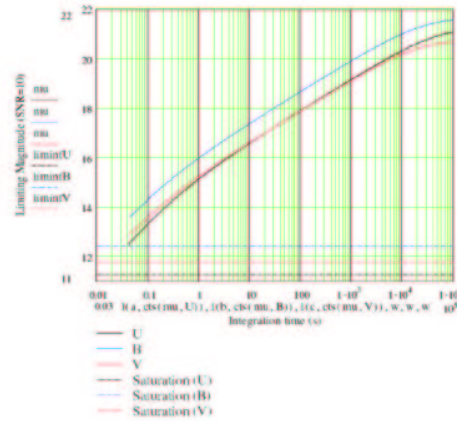


**Fig. 3.** Limiting magnitude versus integration time for SNR=10.

sen among the faintest in the Landolt fields (Landolt 1992), in the U, B, V, R bands. These data have been used for calibrating the detector in the Johnson photometric system (Fig.2). The results of the calibrations have been used to evaluate the sensitivity of the system at the focus of the Cima Ekar telescope: the plot in Fig.3 gives the limiting magnitude (for a Signal to Noise Ratio of 10) in UB V bands versus the integration time. To evaluate the timing performance, we observed the Crab nebula and its 33 ms pulsar. The image in Fig.4 has been obtained from 3 exposition in U, B and V bands, each one 5 minutes long, combined in a single RGB image. A 20 minutes exposure in U band has been taken with the high time resolution mode and a photon list with timing information has been extracted selecting the photons of the Crab Pulsar inside a radius of 1.7 arcsec. The FFT spectrum is shown in Fig.5: the three highest peaks correspond to the spin period and the first two harmonics. The aliased third and fourth harmonics are also apparent. Note that FFT analysis on a segment of the photon list, corresponding to a 4s exposure, was able to reveal the spin modulation of the pulsar with a confidence level of 98%. Obviously, the Crab

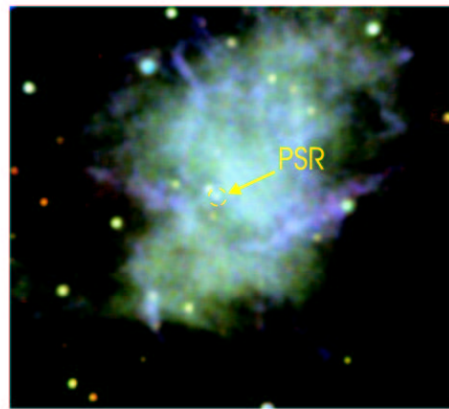


**Fig. 4.** RGB image of the Crab nebula. The pulsar is marked with a circle.

Pulsar is a quite favorable case. However, experimental data from Crab can be used as a template to evaluate the detectability of other sources.

With the aim to investigate the possibility to use the detector to identify the optical counterparts of X/γ-Ray variable sources of known periodicity by detecting optical modulation at the same frequency, we performed a search of periodic emission in the area of the 3C58 SuperNova Remnant (1 hour exposure). A box of 256 × 256 pixel around the SNR has been

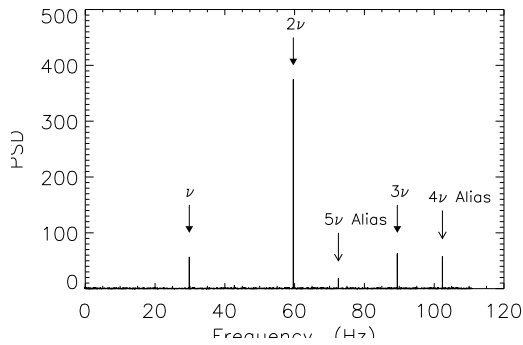


**Fig. 5.** FFT Power Spectrum of the Crab Pulsar light curve.

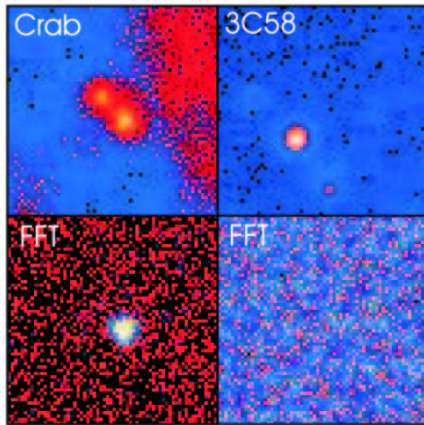


**Fig. 6.** Searching for periodical emission in Crab (left side) and 3C58 (right side) SNRs. Top panels: images of the analyzed area; bottom panels: space-resolved bidimensional view of the FFT power associated with the frequency to be searched for (see text for details).

selected and subdivided in  $64 \times 64$  windows, each one including  $4 \times 4$  pixels ( $=0.42 \times 0.42$  arcsec). For each window, a list of arrival times has been extracted for the photons occurring in that window; then, a FFT power spectrum has been computed and the power associated with the frequency of the pulsar has been recorded, generating a bidimensional array in which each element  $(i,j)$  represents the FFT power, at the frequency to be searched for, of the time serie of the photons coming from the window in position  $(i,j)$ . A source modulated with suitable period (65 ms) should produce a cluster of “high power points”. The right side of Fig.6 shows the results of this analysis for 3C58: no power peaks are found at the period of its pulsar. The same analysis has been performed on the area of the Crab pulsar, searching for the 33 ms period (10 minutes observation). The detection is clearly positive, as it can be seen in the left part of Fig.6.

*Acknowledgements.* We are grateful to Enrico Mattaini and Salvo Incorvaia for the mechanical support. We also wish to thanks Gian Carlo Conti for helping with the laboratory characterization setup.

## References

- Uslenghi, M., Fiorini & Sarri, G. 2004, NIM A, **518**, 223
- Bergamini P. et al. 2000, RSI, **71**, n.4, 1841
- Landolt A. U., 1992, *AJ* **104** (1), 340